

X-Ray Spectral Study of M31 with Ginga

Kazuo MAKISHIMA and Takaya OHASHI

*Department of Physics, Faculty of Science, The University of Tokyo,
3-1, Hongo 7-chome, Bunkyo-ku, Tokyo 113*

Kiyoshi HAYASHIDA, Hajime INOUE, Katsuji KOYAMA,*
Shirou TAKANO,* Yasuo TANAKA, and Atsumasa YOSHIDA

*Institute of Space and Astronautical Science,
1-1, Yoshinodai 3-chome, Sagami-hara-shi, Kanagawa 229*

Martin J. L. TURNER, Huw D. THOMAS, Gordon C. STEWART,
and Rees O. WILLIAMS

*X-Ray Astronomy Group, Department of Physics, University of Leicester,
University Road, Leicester LE1 7RH, U.K.*

and

Hisamitsu AWAKI and Yuzuru TAWARA

*Department of Astrophysics, School of Science, Nagoya University,
Furo-cho, Chikusa-ku, Nagoya 464-01*

(Received 1988 September 2; accepted 1989 January 25)

Abstract

The Andromeda Galaxy M31 was observed in 2–20-keV X-rays with the large Area Counter (LAC) on board Ginga. It was detected at about 2.2-mCrab intensity. After an aspect correction, the 2–20-keV luminosity was estimated to be $5 \times 10^{39} \text{ erg s}^{-1}$ at a distance of 0.7 Mpc. The observed X-ray spectrum is practically indistinguishable from those of Galactic low-mass X-ray binaries. These results were compared closely with the imaging results in soft X-rays from the Einstein Observatory. It was then concluded that the low-mass X-ray binaries dominate the X-ray emission from M31. The integrated X-ray pulsar luminosity in 2–20 keV was estimated to be $< 1.5 \times 10^{39} \text{ erg s}^{-1}$. Contribution from diffuse X-ray components seems insignificant ($< 20\%$) at least in this energy band.

Key words: M31; Normal galaxies; X-ray binaries; X-ray spectra.

1. Introduction

X-ray emission from normal galaxies serves as a tracer for most energetic

* Present address: Department of Astrophysics, School of Science, Nagoya University Furo-cho, Chikusa-ku, Nagoya 464-01.

astrophysical processes taking place in them [for a review, see Long and Van Speybroeck (1983), hereafter referred to as LV83, and Fabbiano (1986, 1989)]. The origin of their X-ray emission, however, can be quite complex and we must incorporate spatial, spectroscopic and temporal information to understand it. The spiral galaxy M31 (Andromeda Galaxy, NGC 224), established as a ~ 2 -mCrab X-ray source (4U 0037+39/2A 0040+409/1H 0039+408), is particularly important for this purpose: its proximity (0.7 Mpc) and resemblance to the Galaxy, combined with the detailed knowledge at various wavelengths, make M31 an ideal prototype for the X-ray study of normal spiral galaxies in reference to the Milky Way.

The Einstein observation of M31 was indeed epoch making. The X-ray emission was resolved into 69 point sources moderately concentrating toward the nucleus (Van Speybroeck et al. 1979, hereafter VS79), and the number of detected sources later increased to 117 (Van Speybroeck and Bechtold 1981, hereafter VB81). Some of these sources were later detected also with EXOSAT (McKee et al. 1984). About 20 of the Einstein sources have been identified with globular clusters (VB81; LV83; Crampton et al. 1984). Fabbiano et al. (1987; hereafter FTV87) showed that the combined Einstein IPC/MPC spectra are represented by a thin-thermal model of temperature 6–13 keV. Thus the Einstein imaging and spectral results on M31 consistently indicate the dominance of the flux from low-mass X-ray binaries (LMXBs; population II close binaries consisting of low-mass stars and non-magnetized neutron stars). However, spectral information has remained rather poor above 3 keV where LMXB-like sources would emit significant energy flux.

Using the Large Area Proportional Counter (LAC; Turner et al. 1989) on board the satellite Ginga [meaning galaxy in Japanese; Makino and the ASTRO-C team (1987)], we obtained for the first time a detailed 2–20-keV X-ray spectrum of M31. As shown in section 3 the spectrum is in fact quite similar to those of the Galactic LMXBs. In section 4 we compare it in detail with the Einstein Observatory results, followed by a discussion in section 5.

2. Observations

The present LAC observation of M31 was performed from 1987 June 16.60 to 17.45, UT, and from 17.69 to 18.48. Excluding periods of Earth occultation, high particle background and solar X-ray contamination, about 10^4 s of net exposure was achieved. Figure 1 shows the position and orientation of the LAC field of view during the observation, superimposed on the Einstein map of M31 (VS79). Thus the LAC field of view (about $1^\circ \times 2^\circ$ FWHM) covered a significant part of the visible galaxy. The following results all concern the X-ray emission spatially integrated over this field of view.

The source was detected at 2.2 ± 0.2 -mCrab (or 24 ± 2 counts s^{-1}) intensity over the 2–20-keV band. This value agrees well with the results of previous non-imaging observations in similar energy bands from Uhuru (2.5 mCrab in 2–6 keV; Forman et al. 1978), Ariel V (2.0 mCrab in 2–18 keV; McHardy et al. 1981) and HEAO-A1 (2.1 mCrab in 0.5–25 keV; Wood et al. 1984). No intrinsic time variation was found during the Ginga observation.

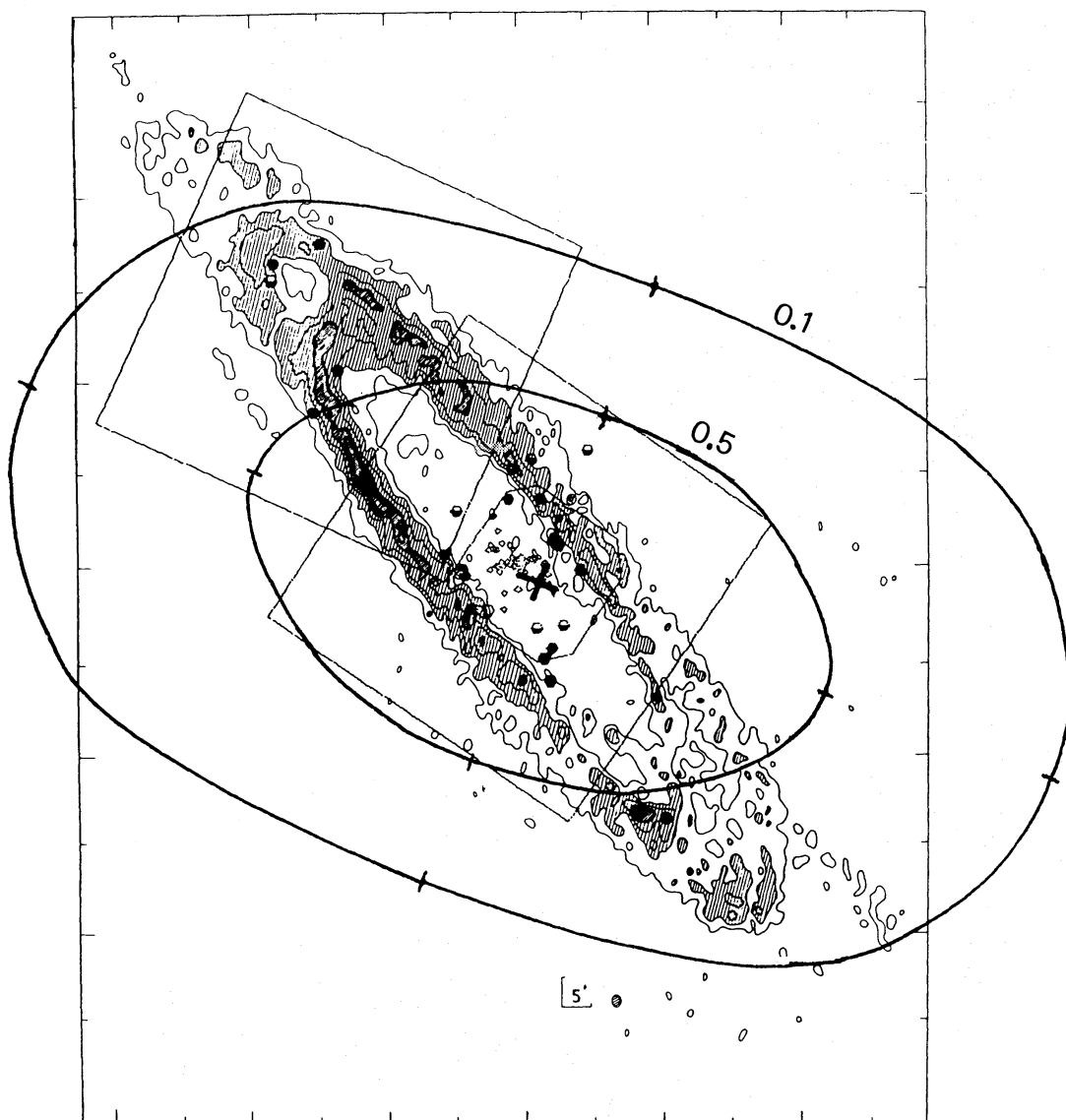


Fig. 1. The LAC field of view during the present observation, superimposed on the H I map of M31 by Emerson (1976), where the Einstein X-ray sources are also indicated (Van Speybroeck et al. 1979). The LAC field center is shown by a cross, together with the 50% and 10% transmission contours.

Figure 2a shows the raw X-ray pulse-height spectrum from M31 obtained after a standard background subtraction. (The background data were taken on 1987 June 15, in a nearby blank sky.) Figure 2b represents the inferred incident spectrum, deconvolved from the detector response using the best-fit LMXB model discussed later. It implies a raw 2–20-keV energy flux of $(6.5 \pm 0.5) \times 10^{-11} \text{ erg s}^{-1} \text{ cm}^{-2}$ incident on the detector.

Employing the source list of Crampton et al. (1984) and assuming equal X-ray intensities of the sources for simplicity, we next calculated the average transmission of the present LAC field of view (figure 1) for the M31 sources. It turned out to be about 0.8. Correcting for this value, the total 2–20-keV energy flux from M31 is estimated to be $(8.1 \pm 0.7) \times 10^{-11} \text{ erg s}^{-1} \text{ cm}^{-2}$. At the 0.7-Mpc distance this gives the 2–20-keV

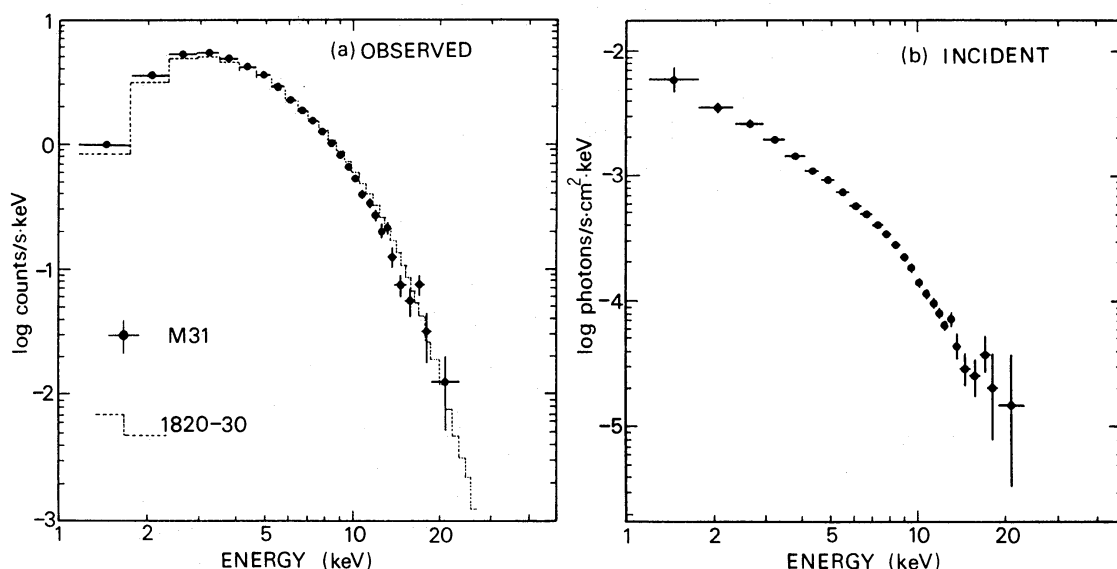


Fig. 2. X-ray spectrum of M31 observed with Ginga LAC. (a) Observed raw X-ray pulse-height spectrum. The dotted histogram shows a spectrum of 4U 1820–30, a typical Galactic LMXB, observed with the same instrument on 1987 May 2. It has been scaled to 1/480 in intensity. (b) Inferred incident photon spectrum deconvolved from the detector response using the best-fit LMXB model of figure 3b (but not corrected for the interstellar absorption). The absorption affects only the lowermost energy channel of the spectrum by <10%.

luminosity of $(4.8 \pm 0.4) \times 10^{39} \text{ erg s}^{-1}$. As shown later, these values are essentially unaffected by the interstellar absorption.

3. Data Analysis and Results

3.1. Spectral Fitting with Thin-Thermal Models

To study the spectral properties, we fitted the observed M31 spectrum first with thin-thermal model [with a Gaunt factor by Gould (1980)] together with absorption by neutral column N_{H} . The results are summarized in table 1. A fairly good fit was obtained with temperature $kT = 7.2 \pm 0.4 \text{ keV}$, where k is the Boltzmann constant. This is consistent with the Einstein value ($kT = 6\text{--}13 \text{ keV}$; FTV87). It implies that the M31 spectrum is harder than those for supernova remnants (SNRs) and coronal sources (typically $kT = 1\text{--}4 \text{ keV}$), while softer than those for X-ray pulsars. Among the known classes of Galactic X-ray sources, the LMXBs exhibit X-ray spectra most similar to that of M31. A power-law continuum with high-energy cutoff gave a still better fit (table 1).

The values of N_{H} required by these thin-thermal and power-law fits (table 1) are however almost an order of magnitude larger than the value $N_{\text{H}} = (5\text{--}8) \times 10^{20} \text{ cm}^{-2}$ established by Einstein Observatory (VS79; FTV87), which is consistent with the line-of-sight absorption within our Galaxy toward M31 (A. A. Stark, C. Heils, J. Bally, and R. Linke 1987, private communication). Since N_{H} can be measured much more reliably in the Einstein band (0.5–4 keV) than in 2–20 keV, we next fixed N_{H} at the

Table 1. Results of model fitting to the M31 spectrum.

Model combinations	[TT]		[PL with cutoff]		[DBB + BB]	[DBB + BB + PL]
	Free N_{H}	Fixed N_{H}	Free N_{H}	Fixed N_{H}		
Thin-thermal (TT):						
Normalization A_{ff}	34 ± 2	25 ± 1
Temperature kT_{ff} (keV) ..	7.2 ± 0.4	8.0 ± 0.3
Disk-blackbody (DBB):						
Normalization A_{d}	12 ± 3	23 ± 7
Temperature kT_{d} (keV)	1.18 ± 0.07	0.95 ± 0.07
Blackbody (BB):						
Normalization A_{b}	0.9 ± 0.2	1.8 ± 0.4
Temperature kT_{b} (keV)	2.04 ± 0.07	1.69 ± 0.08
Power-law with cutoff (PL):						
Normalization A_{p}	75 ± 8	48 ± 2	...	2.0 ± 0.4
Photon index	1.9 ± 0.3	1.6 ± 0.4	...	(1.00)
Cutoff energy E_{c} (keV)	6.8 ± 0.5	5.1 ± 0.3	...	(10.0)
Folding energy E_{f} (keV)	8.2 ± 1.0	7.7 ± 0.6	...	25 ± 15
$\log N_{\text{H}}$ (cm^{-2})	21.6 ± 0.1	(20.8)	21.8 ± 0.2	(20.8)	< 21.3	< 21.5
Reduced chi-squared	2.02	3.74	1.08	1.53	1.26	0.84
Degree of freedom	25	26	23	24	23	21

All the errors are single-parameter 90% confidence limits. All the normalizations are in counts $\text{s}^{-1} \text{keV}^{-1}$ for the 4000 cm^2 area, before the aspect correction. Numbers in parenthesis are fixed parameters.

Einstein value ($10^{20.8} \text{ cm}^{-2}$). The power-law and thin-thermal fits then become unacceptable (table 1; see also figure 3a). We therefore conclude that these spectral models can only approximately describe the Ginga spectrum. Probably the models depend somewhat more steeply on X-ray energy E than the actual spectrum (figure 2b) so that they have demanded artificially large values of N_H [see Makishima et al. (1986)].

3.2. Comparison with LMXB Spectra

We next examine whether the M31 spectrum in fact resembles those of LMXBs. Just for a direct comparison, we show in figure 2a a scaled X-ray spectrum of 4U 1820–30 (a typical LMXB in the globular cluster NGC 6624) obtained with the same instrument. Except below 3 keV where the 4U 1820–30 spectrum is somewhat more absorbed, it coincides very well with the M31 spectrum.

To be quantitative, we fitted the M31 spectrum with a model describing the LMXB spectra (Mitsuda et al. 1984; Makishima and Mitsuda 1985; Makishima et al. 1986). The model consists of two components. The softer one, termed disk-blackbody (DBB) radiation, is the integrated emission from an optically thick accretion disk which is expected to form around the nonmagnetized neutron star (Hoshi 1984; Inoue and Hoshi 1987). The harder one is a ~ 2 -keV blackbody (BB) spectrum emitted presumably from the neutron star surface as a result of thermalization of kinetic energy of the accreting

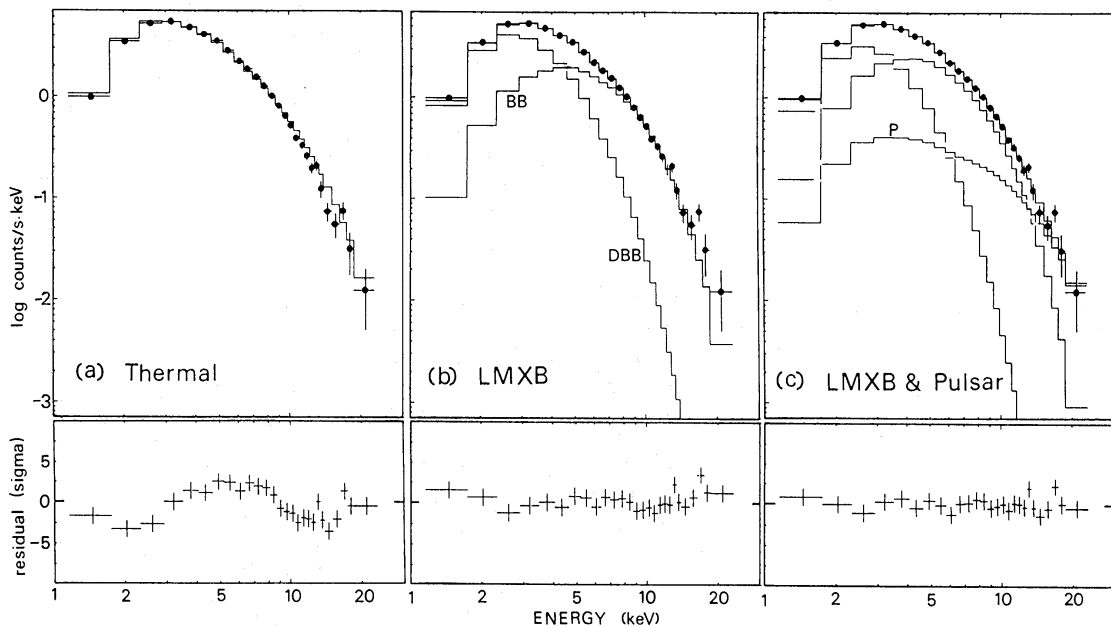


Fig. 3. Results of model fitting to the observed M31 spectrum. The best-fit models have been convolved through the detector response and shown in comparison with the observed pulse-height spectrum of figure 2a. Fit parameters are summarized in table 1. (a) A thin-thermal fit with N_{H} fixed to $10^{20.8} \text{ cm}^{-2}$ (a value determined by the Einstein observation). (b) A fit with disk-blackbody model (denoted DBB) plus blackbody model (denoted BB), which are used to describe the LMXB spectrum. The absorption is left free. See text for details. (c) Similar to panel (a), but including a pulsar-type model (denoted P) as an additional fit component (see text).

matter. The X-ray spectrum of a LMXB is thus described by four parameters; the innermost disk temperature T_{d} and normalization A_{d} for the DBB component, and the temperature T_{b} and normalization A_{b} for the BB component. Bright Galactic LMXBs exhibit narrow scatter both in kT_{b} and kT_{d} , typically $kT_{\text{b}} = 1.8\text{--}2.4 \text{ keV}$ and $kT_{\text{d}} = 1.2\text{--}1.5 \text{ keV}$ (Mitsuda et al. 1984). We therefore expect that the sum spectrum from an assembly of LMXBs can also be expressed as a linear combination of the same two components with these representative temperatures.

With this “DBB + BB” model (plus absorption), an acceptable fit ($\chi^2/\nu = 1.26$ for $\nu = 23$) has been achieved. The best-fit composite model spectrum is shown in figure 3b in comparison with the observed data, and the best-fit parameters are summarized in table 1. The best-fit temperatures ($kT_{\text{b}} = 2.0 \text{ keV}$ and $kT_{\text{d}} = 1.2 \text{ keV}$) are indeed very similar to those for the Galactic LMXBs. The value of N_{H} , $< 2 \times 10^{21} \text{ cm}^{-2}$ (90% confidence limit), is now consistent with the Einstein value (VS79; FTV87). This also ensures that the flux and luminosity values from the present observation (above 2 keV) do not need correction for the absorption. Note that the DBB model scales as $E^{-0.67}$ at $E \ll kT_{\text{d}}$ (Makishima et al. 1986), which is probably closer to the reality than the thin-thermal slope (roughly $\propto E^{-1.3}$ for $E \ll kT$).

The inferred bolometric luminosities of the DBB and the BB components are of the same order, $(3.9 \pm 0.3) \times 10^{39}$ and $(3.0 \pm 0.4) \times 10^{39} \text{ erg s}^{-1}$ respectively after the aspect correction, in agreement with the results for Galactic LMXBs and also with the

prediction of the virial theorem that these two values should be about equal (Mitsuda et al. 1984).

3.3. Possible Contribution from X-Ray Pulsars

We would expect binary X-ray pulsars to give a finite contribution to the M31 X-ray emission. Since their spectra are much harder and often more absorbed than those from LMXBs, we may be able to isolate a pulsar-like component from the observed spectrum. For this purpose we repeated the spectral fitting including the following function $f_p(E)$, so called power-law model with exponential cutoff, as an additional model component which approximates the photon-number spectrum of X-ray pulsars (White et al. 1983):

$$f_p(E) = \begin{cases} A_p E^{-\alpha} \exp(-\sigma N_H), & \text{for } E < E_c \\ A_p E^{-\alpha} \exp[-\sigma N_H - (E - E_c)/E_f], & \text{for } E > E_c. \end{cases} \quad (1)$$

Here σ is the interstellar photoelectric absorption coefficient, while A_p , α , E_c , and E_f are free parameters. To avoid strong couplings among these fit parameters, we fixed α at 1.0 and E_c at 10.0 keV, thus leaving A_p and E_f free.

As shown in figure 3c and table 1 the fit has actually been improved by inclusion of this additional model, and optimized when $f_p(E)$ carries $25 \pm 5\%$ of the observed flux at 10 keV. We prefer, however, to treat these as modest upper limits, because LMXB themselves show some excess over the DBB+BB model above 15–20 keV (Mitsuda et al. 1984) presumably due to Comptonization. Thus the 90% confidence upper limit on the relative pulsar flux will be quoted to be 30% at 10 keV, and 10% at 2 keV. After the aspect correction, these values imply the 2–20-keV pulsar luminosity of $< 1.0 \times 10^{39} \text{ erg s}^{-1}$ ($< 1/5$ of the estimated total 2–20-keV luminosity). Considering however that the massive binaries must be distributed along the spiral arms of M31 and hence rather away from the LAC view center, a somewhat larger aspect correction factor may be appropriate. A safer upper limit therefore may be about $1.5 \times 10^{39} \text{ erg s}^{-1}$.

To search for regular pulsations from the brightest X-ray pulsars in M31, we performed a standard Fourier power-spectrum analysis over the period range of 1–128 s using the 4.6–18.5-keV data. However none was found. The 95% confidence upper limit to the peak-to-peak amplitude of any sinusoidal modulation over this period range is 1.7% of the mean X-ray flux. The corresponding upper limit to the peak-to-peak luminosity modulation is $8 \times 10^{37} \text{ erg s}^{-1}$. Since this value is still somewhat larger than those of typical bright X-ray pulsars in the Galaxy (a few times $10^{37} \text{ erg s}^{-1}$; Bradt and McClintock 1983), the present nondetection is not surprising.

3.4. Upper Limits to Thin-Thermal Components

The M31 spectrum may also have contributions from an assembly of low-luminosity point sources (white dwarfs, RS CVn systems etc.) as well as hot gaseous components such as SNRs and galactic halo (LV83). We will call them thin-thermal sources (TTS) and treat them together, as they exhibit thin-thermal spectra with temperatures of a few keV. The ridge X-ray emission along the Milky Way, with integrated luminosity of $L_x \sim 10^{38} \text{ erg s}^{-1}$ (Warwick et al. 1985; Koyama et al. 1986),

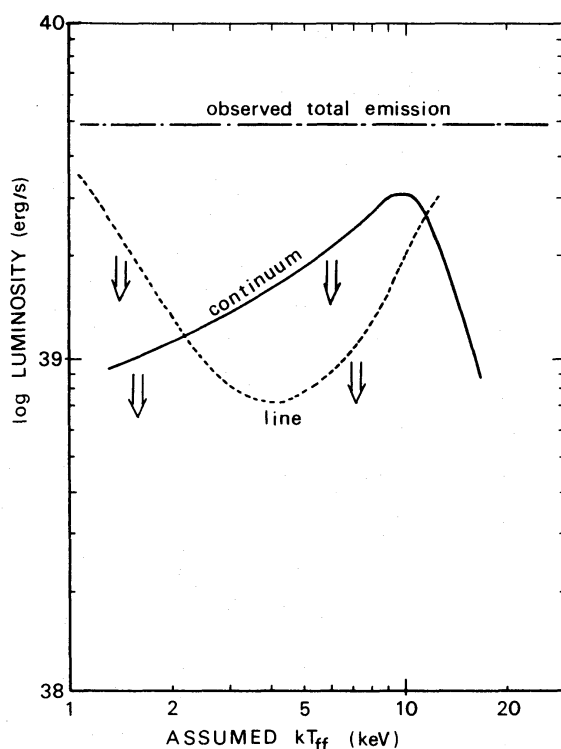


Fig. 4. Upper limits to the 2–20-keV luminosity of thin-thermal emission component in M31, plotted against the assumed thin-thermal temperature kT_{ff} . The dotted curve is an estimate based on the observed upper limit to the iron-line equivalent width, in comparison with the theoretical calculation assuming cosmic abundance of iron and ionization equilibrium. The solid curve was derived from a combined thin-thermal plus LMXB fit to the continuum with N_{H} fixed to $10^{20.8} \text{ cm}^{-2}$.

should also be included here, although it is still unclear if this itself is the sum of other TTS or not. Since these thin-thermal spectra are similar in shape to the LMXB spectra, an estimation of their contribution to the M31 spectrum is not trivial. Accordingly we conducted the following two attempts to estimate it.

Firstly we tried a spectral fitting incorporating the LMXB model and the thin-thermal model together, but fixing N_{H} to $10^{20.8} \text{ cm}^{-2}$ (the Einstein value) and kT_{b} to 2.0 keV (a canonical value). Assuming various values for the thin thermal temperature T_{ff} , we examined the intensity allowed for the TTS component. The fit has somewhat been improved by inclusion of thin thermal model for $2 < kT_{\text{ff}} < 12 \text{ keV}$, but again we utilize this information only to set conservative upper limits to the 2–20-keV luminosity of the TTS component. As summarized in figure 4, this argument can only weakly constrain the TTS contribution, especially for values of kT_{ff} close to the best-fit temperature (7–8 keV) associated with the thin-thermal fit (figure 3a).

Secondly, the TTS spectra usually show an intense iron K-emission line at 6.7 keV [mainly from He-like iron ions; e.g., Makishima (1986)]. Calculations assuming ionization equilibrium and cosmic abundances predict the iron-line equivalent width (EW) to be 0.5–1.1 keV, for plasma temperatures in the range 1–10 keV, although the observed values of the iron-line EW often deviate from the calculations (Koyama 1988). We accordingly fitted the observed spectrum with the DBB + BB model plus a Gaussian

model (with 0.1-keV FWHM and 6.7-keV line-center energy), the latter simulating the iron emission line. This analysis has constrained the line equivalent width (EW) to <80 eV at the 90% confidence limit. In figure 4 we translate this result into upper limits to the 2–20-keV luminosity of the thin-thermal component. Incidentally the LMXBs themselves emit 6.7-keV iron lines with EW of several tens electronvolts (Suzuki et al. 1984; White et al. 1986; Hirano et al. 1987), with which the present result is consistent.

From figure 4 we presume that the TTS contribute at most 20% to the 2–20-keV luminosity of M31, if the typical TTS temperature is in the range 1–7 keV and if the iron line EW is close to the expected value. The upper limit however becomes less restrictive if the thin-thermal temperature is in the range 7–15 keV and/or the iron line EW is somehow suppressed.

4. Comparison with the Einstein Observatory Results

All the Einstein point sources in M31 sum up to give a 0.5–4.5-keV luminosity of about $3.6 \times 10^{39} \text{ erg s}^{-1}$, after correcting for $N_{\text{H}} = 10^{20.8} \text{ cm}^{-2}$ (VS79; VB81; LV83). For comparison, we have extrapolated the Ginga spectrum toward <2 keV, using the best-fit DBB + BB model (figure 2b). This has given the unabsorbed luminosity estimate of $(3.3 \pm 0.5) \times 10^{39} \text{ erg s}^{-1}$ over the same 0.5–4.5-keV range. Thus the two observations are in good agreement, but they are possibly based on different samples in the luminosity distributions of the M31 X-ray sources. The agreement therefore would be only by chance unless this difference in source sampling is shown to have negligible effect.

The Ginga spectrum integrates over the entire luminosity function, while the Einstein sample is limited to luminous ($L_{\text{x}} > 10^{37} \text{ erg s}^{-1}$) point-like sources (LMXBs, pulsars, active nucleus etc.). Most TTS are thus excluded from the Einstein sample, but they do not contribute very much either to the Ginga spectrum (see section 3.4). Therefore the two results are consistent in this respect. As to LMXBs, the luminosity function of globular cluster X-ray sources in Our Galaxy (Hertz and Grindlay 1983) implies that sources with $L_{\text{x}} < 10^{37} \text{ erg s}^{-1}$ contribute only $<10\%$ to the total luminosity. By analogy, we presume that LMXBs in M31 which are below the Einstein detection limit ($\sim 10^{37} \text{ erg s}^{-1}$) have little effect upon the Ginga spectrum. X-ray pulsars must also be considered. Their hard spectra, large intrinsic absorption, and luminosity distribution extending well below the Einstein limit, all tend to increase the downward extrapolated Ginga luminosity relative to the Einstein value. However, considering that the downward extrapolation of the Ginga spectrum relies mostly on the observed flux at 2–3 keV, and that the pulsar flux has already been estimated to $<10\%$ of the total flux at 2 keV (see section 3.3), X-ray pulsars would cause a difference between the two luminosity values of no more than 10%. Finally, one X-ray source possibly associated with the M31 nucleus is at most $10^{38} \text{ erg s}^{-1}$ in luminosity (LV83) and can be neglected here.

From the above arguments, we conclude that both the Einstein and Ginga luminosities are based on an almost identical source sample, namely bright LMXBs. This confirms the physical meanings of the agreement between the two experiments, suggesting that the DBB + BB model reasonably represents the LMXB spectra not only

in the original Ginga band (2–20 keV) but also in the soft X-ray range (see also FTV87). Note that the 0.5–4.5-keV luminosity estimate increases by about 30% if we extrapolate the Ginga spectrum using the thin-thermal fit, which has a steeper energy dependence than the DBB model.

As reported by FTV87, the combined Einstein IPC/MPC spectra from the central region of M31 can be represented by a thin-thermal model with temperature 6–13 keV. Considering that the Ginga spectrum can be approximated by a thin-thermal model (figure 3a), it is reasonable to expect that the data from the MPC (with a factor 6 smaller effective area and a much coarser energy binning than the Ginga LAC) can be represented adequately with a thin-thermal model.

5. Discussion and Conclusion

We have shown that the 2–20-keV X-ray luminosity of M31 is about $5 \times 10^{39} \text{ erg s}^{-1}$. By analyzing the Ginga spectrum, we have concluded that the LMXBs provide a major contribution to the 2–20-keV X-ray emission from M31. This reconfirms the conclusion previously obtained with the Einstein Observatory. Such a dominance of LMXBs has already been established in our Galaxy; the integrated LMXB luminosity in our Galaxy may be $(1\text{--}2) \times 10^{39} \text{ erg s}^{-1}$. Compared with our Galaxy, M31 has about twice larger mass and a far higher X-ray source density in the bulge region (VS79; LV83), and is richer in Population II objects (globular clusters etc.). Moreover the individual globular-cluster X-ray sources in M31 seem brighter in X-rays than those in the Milky Way (VB81; LV83). The present result seems a natural consequence of all these facts.

We have estimated the integrated luminosity of X-ray pulsars to be $\lesssim 1.5 \times 10^{39} \text{ erg s}^{-1}$. This is roughly consistent with the Einstein results that the integrated luminosity of the sources in the arm region is $(1\text{--}1.5) \times 10^{39} \text{ erg s}^{-1}$ in 0.5–4.5 keV (VS79; VB81). For comparison the total pulsar luminosity in our Galaxy may be a few times $10^{38} \text{ erg s}^{-1}$. Therefore, in both galaxies the LMXBs seem to have integrated luminosities a few times larger than those for massive X-ray binaries. However, we must keep in mind that X-ray pulsars in the Magellanic Clouds have very large luminosities [a few times $10^{38} \text{ erg s}^{-1}$ individually; Clark et al. (1978) and Bradt and McClintock (1983)].

The hot gaseous components in normal galaxies is an interesting area for studies at X-ray energies. Contribution from such components to the total X-ray flux may be rather small (perhaps <10% in luminosity) in our Galaxy, but can be quite dominant in starburst galaxies (e.g. Watson et al. 1984; Fabbiano 1988) as well as ellipticals (Forman et al. 1985; Trinchieri et al. 1986; Canizares et al. 1987). While the total LMXB luminosity is expected to be roughly proportional to the stellar mass content of each galaxy, the hot diffuse components may reflect more fundamental properties of a normal galaxy as a self-gravitating system, e.g., depth of the gravitational potential, angular momentum, star-forming activities, and so on. It is therefore extremely important to understand the nature of diffuse X-ray emission from galaxies and relate them to various properties of them. The present observations have indicated that such hot diffuse matter is not a major constituent of the X-ray emission from M31. We, however, notice that

the diffuse X-ray emission may become progressively important for galaxies with larger mass and/or higher activities.

The authors are grateful to all the member of the Ginga team. Particular thanks are due to M. Takizawa for his help in data analysis.

References

- Bradt, H. V. D., and McClintock, J. E. 1983, *Ann. Rev. Astron. Astrophys.*, **21**, 13.
- Canizares, C. R., Fabbiano, G., and Trinchieri, G. 1987, *Astrophys. J.*, **312**, 503.
- Clark, G., Doxsey, R., Li, F., Jernigan, J. G., and van Paradijs, J. 1978, *Astrophys. J. Letters*, **221**, L37.
- Crampton, D., Cowley, A. P., Hutchings, J. B., Schade, D. J., and Van Speybroeck, L. P. 1984, *Astrophys. J.*, **284**, 663.
- Emerson, D. T. 1976, *Monthly Notices Roy. Astron. Soc.*, **176**, 321.
- Fabbiano, G. 1986, *Publ. Astron. Soc. Pacific*, **98**, 525.
- Fabbiano, G. 1988, *Astrophys. J.*, **330**, 672.
- Fabbiano, G. 1989, *Ann. Rev. Astron. Astrophys.*, **27**, in press.
- Fabbiano, G., Trinchieri, G., and Van Speybroeck, L. S. 1987, *Astrophys. J.*, **316**, 127 (FTV87).
- Forman, W., Jones, C., Cominsky, L., Julien, P., Murray, S., Peters, G., Tananbaum, H., and Giacconi, R. 1978, *Astrophys. J. Suppl.*, **38**, 357.
- Forman, W., Jones, C., and Tucker, W. 1985, *Astrophys. J.*, **293**, 102.
- Gould, R. J. 1980, *Astrophys. J.*, **238**, 1026.
- Hertz, P., and Grindlay, J. E. 1983, *Astrophys. J.*, **275**, 105.
- Hirano, T., Hayakawa, S., Nagase, F., Masai, K., and Mitsuda, K. 1987, *Publ. Astron. Soc. Japan*, **39**, 619.
- Hoshi, R. 1984, *Publ. Astron. Soc. Japan*, **36**, 785.
- Inoue, H., and Hoshi, R. 1987, *Astrophys. J.*, **322**, 320.
- Koyama, K. 1988, in *Physics of Neutron Stars and Black Holes*, ed. Y. Tanaka (Universal Academy Press, Tokyo), p. 55.
- Koyama, K., Makishima, K., Tanaka, Y., and Tsunemi, H. 1986, *Publ. Astron. Soc. Japan*, **38**, 121.
- Long, K. S., and Van Speybroeck, L. P. 1983, in *Accretion Driven Stellar X-Ray Sources*, ed. W. H. G. Lewin and E. P. J. van den Heuvel (Cambridge University Press, Cambridge), p. 117 (LV83).
- Makino, F., and the ASTRO-C team 1987, *Astrophys. Letters Commun.*, **25**, 223.
- Makishima, K. 1986, in *The Physics of Accretion onto Compact Objects*, ed. K. O. Mason, M. G. Watson, and N. E. White (Springer-Verlag, Berlin), p. 249.
- Makishima, K., Maejima, Y., Mitsuda, K., Bradt, H. V., Remillard, R. A., Tuohy, I. R., Hoshi, R., and Nakagawa, M. 1986, *Astrophys. J.*, **308**, 635.
- Makishima, K. and Mitsuda, K. 1985, in *Proc. Japan-US Seminar on Galactic and Extragalactic Compact X-ray Sources*, ed. Y. Tanaka and W. H. G. Lewin (Institute of Space and Astronautical Science, Tokyo), p. 127.
- McHardy, I. M., Lawrence, A., Pye, J. P., and Pounds, K. A. 1981, *Monthly Notices Roy. Astron. Soc.*, **197**, 893.
- McKechnie, S. P., Jansen, F. A., de Korte, P. A. J., Hulscher, F. W. H., van der Klis, M., Bleeker, J. A. M., and Mason, K. O. 1984, in *X-ray Astronomy '84*, ed. M. Oda and R. Giacconi (Institute of Space and Astronautical Science, Tokyo), p. 373.
- Mitsuda, K., Inoue, H., Koyama, K., Makishima, K., Matsuoka, M., Ogawara, Y., Shibasaki, N., Suzuki, K., Tanaka, Y., and Hirano, T. 1984, *Publ. Astron. Soc. Japan*, **36**, 741.
- Suzuki, K., Matsuoka, M., Inoue, H., Mitsuda, K., Ohashi, T., Tanaka, Y., Hirano, T., and Miyamoto, S. 1984, *Publ. Astron. Soc. Japan*, **36**, 761.
- Trinchieri, G., Fabbiano, G., and Canizares, C. R. 1986, *Astrophys. J.*, **310**, 637.
- Turner, M. J. L., Thomas, H. D., Patchett, B. E., Reading, D. H., Makishima, K., Ohashi, T., Dotani, T., Hayashida, K., Inoue, H., Kondo, H., Koyama, K., Mitsuda, K., Ogawara, Y., Takano, S., Awaki, H.,

- Tawara, Y., and Nakamura, N. 1989, *Publ. Astron. Soc. Japan*, **41**, 345.
- Van Speybroeck, L., and Bechtold, J. 1981, in *X-ray Astronomy with the Einstein Satellite*, ed. R. Giacconi (D. Reidel Publishing Company, Dordrecht), p. 153 (VB81).
- Van Speybroeck, L., Epstein, A., Forman, W., Giacconi, R., Jones, C., Liller, W., and Smarr, L. 1979, *Astrophys. J. Letters*, **234**, L45 (VS79).
- Warwick, R. S., Turner, M. J. L., Watson, M. G., and Willingale, R. 1985, *Nature*, **317**, 218.
- Watson, M. G., Stanger, V., and Griffiths, R. E. 1984, *Astrophys. J.*, **286**, 144.
- White, N. E., Peacock, A., Hasinger, G., Mason, K. O., Manzo, G., Taylor, B. G., and Branduradi-Raymont, G. 1986, *Monthly Notices Roy. Astron. Soc.*, **218**, 129.
- White, N. E., Swank, J. H., and Holt, S. S. 1983, *Astrophys. J.*, **270**, 711.
- Wood, K., Meekins, J. F., Yentis, D. J., Smathers, H. W., McNutt, D. P., Bleach, R. D., Byram, E. T., Chubb, T. A., Friedman, H., and Meidav, M. 1984, *Astrophys. J. Suppl.*, **56**, 507.